

See discussions, stats, and author profiles for this publication at: <https://www.researchgate.net/publication/229440893>

Real time kinetics and thermochemistry of the uptake of HCl, HBr and HI on water ice in the temperature range 190 to 210 K

ARTICLE in BERICHTE DER BUNSENGESELLSCHAFT/PHYSICAL CHEMISTRY CHEMICAL PHYSICS · JULY 1998

DOI: 10.1002/bbpc.19981020704

CITATIONS

20

READS

26

4 AUTHORS, INCLUDING:



[Michel J Rossi](#)

Paul Scherrer Institut

259 PUBLICATIONS 6,478 CITATIONS

[SEE PROFILE](#)

Real Time Kinetics and Thermochemistry of the Uptake of HCl, HBr and HI on Water Ice in the Temperature Range 190 to 210 K

Benoît Flückiger, Axel Thielmann, Lukas Gutzwiller and Michel J. Rossi *)

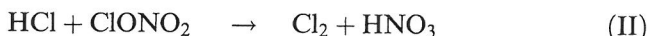
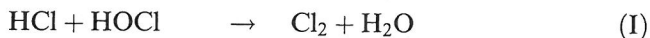
Laboratory of Air and Soil Pollution Studies (LPAS), Département de Génie Rural (DGR), Swiss Federal Institute of Technology (EPFL), CH-1015 Lausanne, Switzerland

Key Words: Chemical Kinetics / Heterogeneous Chemical Reactions / Interfaces / Mass Spectrometry / Surfaces

The real time kinetics of adsorption and desorption of HCl on ice have been studied in a very low pressure reactor (Knudsen cell). We used two complementary techniques, namely pulsed valve or transient supersaturation and steady state experiments. The kinetics of adsorption, following a first order rate law, has been found to depend on the number of HCl molecules in a pulse for transient supersaturation and on the HCl partial pressure or flow rate in steady state experiments. The uptake coefficient γ ranges from 0.34 to 0.22 in the temperature range 190 to 210 K for dry adsorption leading to a quasi-liquid state of HCl on ice and from 0.31 to 0.13 for adsorption leading to a liquid solution of HCl. In both cases a negative temperature dependence for uptake of HCl on ice of -1.8 ± 0.5 and -3.1 ± 0.5 kcal/mol has been observed. In addition, the fraction of HCl that could be retrieved by desorption after dosage with HCl depended strongly on the thermodynamic state of the HCl/ice substrate as well as on the temperature and varied in the range from 10 to 80%. We determined the rate of irreversible surface-to-bulk loss, with a limiting rate of $1.0 \cdot 10^{-3}$ molecule $s^{-1} cm^{-2}$ at 200 K. In addition, we studied the kinetics of adsorption of HBr and HI on ice resulting in γ values similar to HCl. However, ice in the range 190 to 210 K did not support any measurable vapor pressure of both HBr and HI after adsorption of up to several formal monolayers in contrast to HCl.

Introduction

Heterogeneous processes occurring on polar stratospheric clouds (PSCs) or background atmospheric particulate have been demonstrated to be intimately linked to stratospheric ozone depletion [1]. It has been suggested that the following reactions (I–III) involving hydrogen chloride are responsible for the conversion of chlorine locked into reservoir molecules into photolytically active chlorine. They may occur efficiently if HCl is initially present on the ice surface [2]:



HCl is only sparingly soluble in bulk ice [3]. In order for the heterogeneous processes involving HCl to take place efficiently on PSC's, HCl does not need to be present at high concentrations in the ice matrix: the requirement for reaction is that sufficient HCl is available at the ice surface at the moment of interaction with the other reactant. It is known that HCl vapor has a high affinity for hydration in liquid water. Gas phase hydrogen chloride is converted into hydrochloric acid, a process that is exothermic by approximately 18 kcal/mol [4] when the gas is dissolved in H_2O . However, studies of the liquid-solid partitioning of HCl in aqueous solutions have shown that only very small amounts of HCl are incorporated into the bulk ice phase; the reported partition coefficients range from 10^{-2} to 10^{-7} [3, 5–8]. Although it had once been suggested that ice takes up large amounts of

HCl [2, 9], the measurements of Wolff et al. [10] indicate that HCl concentrates at grain boundaries because the solubility of HCl in ice is small.

Several groups [11, 12] have reported that HCl is being taken up efficiently and in large quantities on the ice surface at partial pressures of approximately 10^{-5} Torr and above ($T=200$ K), but at pressures below about 10^{-6} Torr much smaller amounts are adsorbed, roughly corresponding to a monolayer coverage or less. Laboratory experiments carried out by Molina and co-workers [2] have shown that the HCl partial pressure at the solid-liquid coexistence line is what determines the nature of the uptake process. In fact, surface melting occurs if the partial pressure of HCl exceeds the value given by the coexistence line. They observe that a partial pressure of $5 \cdot 10^{-5}$ Torr leads to monolayer uptake at 250 K resulting in a quasi-liquid state of the HCl in ice. However, the same partial pressure leads to surface melting at 210 K with a higher amount of HCl taken up resulting in a true liquid HCl/ H_2O mixture.

Furthermore, studies on the solubility and diffusion rate of HCl in ice [10, 13] and on the intrinsic surface properties of ice with respect to HCl adsorption [14–16] have been published. Moreover, Gertner and Hynes used molecular dynamics simulations to study the ionization of HCl on an ice surface at 190 K and calculated a change in free energy ranging from -5.8 to -6.7 kcal/mol for various likely initial conditions [17].

Kinetic studies indeed suggest that the rate of surface processes such as adsorption and desorption is so rapid that it is unlikely that surface-to-bulk diffusion may be involved [18]. Oppliger et al. recently showed that the presence of adsorbed HCl, probably in ionized form [19], seems to be necessary for bimolecular heterogeneous reactions, such as reaction (II), to occur on an ice surface.

*) Author to whom correspondence should be addressed.

Heterogeneous activation of HBr is thought to play a minor role due to its small concentration in the atmosphere [20]. Only a few studies on the heterogeneous reaction of HBr exist [11, 21, 22]. The general finding is that HBr reacts more efficiently than HCl on ice which may compensate somewhat for the low abundance. Nevertheless, HBr may accumulate on ice in cases where high particle densities occur, e.g. in clouds or contrails. Currently, very little is known about the interaction of HI on ice in the temperature range of interest. Pickering [23] observed that HI forms hydrates, $\text{HI}\cdot n\text{H}_2\text{O}$ with $n=2, 3, 4$ in the temperature range 190 to 230 K. Chu and Chu [24] conclude from their experiments that both HBr and HI on ice at 188 K are not in a “free” ionic form which is consistent with the formation of hydrates near the ice-film surface.

This paper emphasizes the fundamental study of the kinetics of interaction of HCl with ice from a physicochemical point of view. Real-time experiments on the kinetics of adsorption of HCl on ice have been performed and interpreted using the well known phase diagram of the system HCl/H₂O [8, 25, 26]. In addition, the corresponding desorption rate has been determined in pulsed valve as well as in steady state experiments. The kinetics of adsorption of HBr and HI on ice have been studied using the same techniques.

Experimental Details

The study has been carried out using a low-pressure flow reactor in the molecular flow regime (Knudsen cell). The basic considerations for the use of these reactors have recently been described in detail elsewhere [27–29]. In summary, the flow rate and size of the escape aperture can be chosen to control the density and residence time of the gaseous species, hence the extent of the reaction in the reactor. The total pressure is kept low enough to ensure that the reactor remains in the molecular flow regime. The molecules enter the Knudsen cell flow reactor and effuse out of an orifice after having spent the average lifetime τ inside the reactor during which they underwent several thousand collisions with the Teflon-coated reactor wall. The molecular beam effusing out the escape orifice is modulated and monitored using phase-sensitive electron-impact quadrupole mass spectrometry (QMA). In order to determine the rate of the chemical loss on a given sample surface, a part of the reactor wall is replaced by the surface of interest which can be isolated from the remainder of the reactor by a gas tight plunger. The solid ice sample was obtained by condensation of a measured external flow of water vapor in the range 10^{18} molecule s⁻¹ onto the low temperature support [19] in order to obtain a substrate with a thickness of at least several thousand monolayers (ML). The thickness of the ice sample was calculated from the measured number of H₂O molecules condensed and the bulk density of ice. All the uptake experiments discussed below were performed with an

Table 1
Knudsen cell parameters

| Reactor parameter | Value |
|---|---|
| Volume V | 1830 cm ³ |
| Gas number density | (1–1000) 10^{10} cm ⁻³ |
| Sample area A_s | 15 cm ² |
| Calculated collision frequency ω on sample surface | $1/4 \cdot (8RT/\pi M)^{1/2} \cdot A_s \cdot 1/V = 85.8 \text{ s}^{-1}$ for HCl @ 300 K |
| Experimental escape rate constant k_{esc} | 5.2 s ⁻¹ ($\varnothing=15$ mm) 2.2 s ⁻¹ ($\varnothing=8$ mm) 0.66 s ⁻¹ ($\varnothing=4$ mm) |

external flow of water in order to compensate for net evaporation so that the ice was in equilibrium with its gas phase at the chosen steady state conditions.

Our results presented here were obtained by performing both *pulsed valve* and *steady state* experiments briefly described below.

Pulsed valve experiments

A known number of gas molecules is admitted across a pulsed solenoid valve into the reactor and interacts with the reactive surface. The recorded QMA signal $S(t)$ is a function of time, proportional to the flow of gaseous species out of the reactor and follows a simple exponential decay upon admission of the gas pulse according to

$$S(t) = S_0 \exp(-(k_{\text{esc}} + k_{\text{eff}})t) \quad (1)$$

where $k_{\text{esc}} = 1/\tau$ is the escape rate constant which only depends on the molecular velocity as well as on the geometry of the reactor. Thus $k_{\text{esc}} = (\{c\}/4V) \cdot A_h$ where $\{c\}$ is the average molecular velocity, V the volume of the Knudsen cell and A_h the area of the escape orifice and is experimentally obtained in a *reference* experiment by isolating the reactive surface from the remainder of the reactor. On the other hand, k_{eff} is the rate constant of interest corresponding to the heterogeneous interaction which is competitive with the physical loss of effusion across the escape aperture (k_{esc}). The value of k_{eff} obtained from a *reactive* experiment may be expressed on a per collision basis resulting in an uptake coefficient γ which corresponds to the probability that a molecule interacting with a surface disappears from the gas phase. The uptake coefficient is defined as $\gamma = k_{\text{eff}}/\omega = 4Vk_{\text{eff}}/\{c\}A_s$, where ω is the gas-surface collision frequency of a typical molecule with the area A_s of the sample surface. Typical values of the reactor parameters are given in Table 1. The pulsed valve technique has the advantage that it avoids surface saturation and contamination phenomena to a large degree in view of the small doses dispensed, which lie in the range of 5% of a monolayer to several formal monolayers of HCl on ice corresponding to $3 \cdot 10^{14}$ to $5 \cdot 10^{16}$ molecules per pulse, respectively.

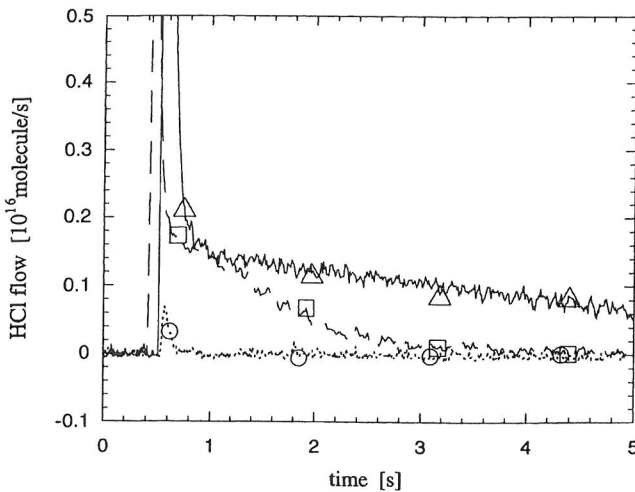


Fig. 1

Pulsed valve experiment of HCl interacting with an ice sample at 200 K. The decay of the HCl signal is followed for three different doses: $3.6 \cdot 10^{14}$ molecules (open circles), $3.3 \cdot 10^{15}$ molecules (open squares) and $1.1 \cdot 10^{16}$ molecules (open triangles). Escape aperture: 15 mm

Steady State Experiments

In this type of experiment, a continuous and constant flow F_i of HCl enters the reactor. Assuming that the rate law for adsorption of HCl is first order, simple steady-state considerations lead to the following expression for the first order rate constant $k_{\text{uni}} = ((S_0/S) - 1) \cdot k_{\text{esc}}$, where S_0 and S correspond to the MS signal with the sample isolated (S_0) and exposed to the gas flow (S), respectively. By using this technique, we are able to follow the interaction of the gas phase with the reactive surface on a long time scale and also confirm the results obtained in pulsed valve experiments.

Results and Discussion

Pulsed Valve Experiments

Real time kinetics of the adsorption of HCl on ice from transient supersaturation experiments.

We performed pulsed valve experiments in which we exposed given doses of HCl to a fresh ice sample covering the range between 10^{14} and 10^{16} molecules per pulse. We observe the formation of a steady state HCl signal as a function of increasing dose after a fast exponential drop (Fig. 1). As this HCl signal essentially remains constant for a few seconds for a sufficiently high dose, we interpret it as a steady state level (Fig. 2). The signal subsequently decreases to its initial background level, after a duration which is proportional to the injected dose. In fact, the HCl signal level is at steady state for the 4 and 8 mm orifices (corresponding to a gas residence time τ of 1.5 and 0.45 s, respectively) while it decreases slightly when using the 15 mm orifice ($\tau=0.2$ s) owing to the fact that the pumping speed ($k_{\text{esc}} \cdot V$) is large and the quantity

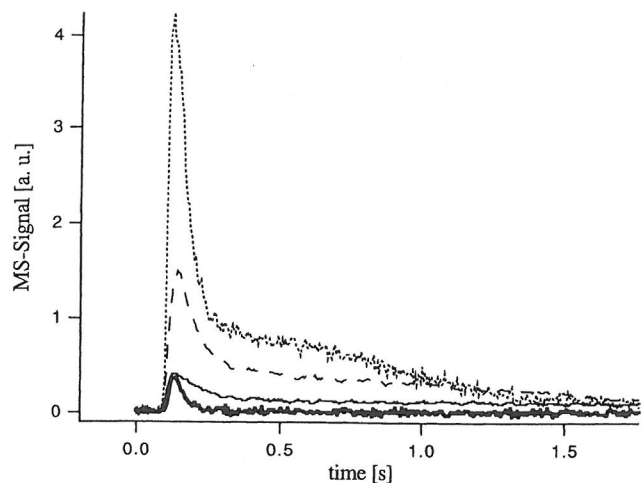


Fig. 2

HCl signals pertaining to reactive pulses at $T=210$ K interacting with pure ice and observation of the transition from slowly decaying to steady state levels of HCl as a function of increasing residence time. The bold solid line corresponds to a pulse at a low dose of $6 \cdot 10^{14}$ molecules (15 mm orifice). The pulses at a high dose of $8 \cdot 10^{15}$ molecules using the 15, 8 and 4 mm orifice represented by the top dotted line, middle dashed line and lower solid line, respectively, attain the slowly decaying (top) and the steady state level (second and third from the top)

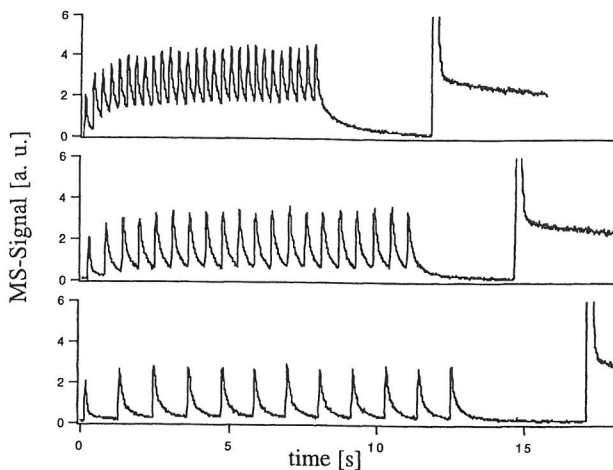


Fig. 3

Raw data from a typical Repetitive Pulse Experiment (RPE) performed at $T=200$ K. The injection frequencies are 3.3 Hz (upper trace), 1.66 Hz (middle trace) and 0.91 Hz (lower trace). The reference dose (not shown here) corresponds to approximately $8 \cdot 10^{14}$ molecules per pulse. The pulse duration was set at 1 ms for each pulse. After a series of pulses, a larger pulse was dispensed in order to compare the resulting steady state level

of adsorbed HCl too limited to sustain a true steady state of HCl in the Knudsen reactor.

In addition, we performed complementary Repetitive Pulse Experiments (RPE) in which several small pulses of typically $7 \cdot 10^{14}$ molecules are successively and rapidly injected. Fig. 3 displays reactive traces at different intervals of time between each pulse. The height of the observed steady state signal level between the pulses is strongly

Table 2

Steady state levels F_{SS} in the aftermath of a pulse of HCl on fresh ice samples at different orifice sizes (15, 8 and 4 mm diameter). At each temperature the injected dose was identical for the three orifices

| T [K] | Dose [molec] 10(15) | F_{SS} | F_{SS} | F_{SS} |
|-------|---------------------------|--------------------------------|-------------------------------|-------------------------------|
| | | [molec/s] \emptyset 15 mm | [molec/s] \emptyset 8 mm | [molec/s] \emptyset 4 mm |
| | | 10(15) | 10(15) | 10(15) |
| 210 | 5.22 | 3.77 | 1.98 | 7.41 |
| 210 | 5.18 | 3.88 | 2.12 | 6.97 |
| 210 | 5.36 | 3.86 | 1.98 | 7.30 |
| 210 | 5.10 | 3.93 | — | 6.30 |
| 210 | 5.18 | 4.00 | — | 7.73 |
| 210 | 5.16 | 3.96 | — | — |
| 200 | 9.38 | 1.89 | 1.09 | 0.40 |
| 200 | 9.24 | 2.09 | 1.08 | 0.37 |
| 200 | 9.18 | 2.09 | 1.10 | 0.42 |
| 200 | 9.38 | 2.02 | — | 0.41 |
| 200 | 9.16 | 1.93 | — | — |
| 200 | 9.18 | 1.84 | — | — |
| 190 | 7.92 | 0.76 | 0.38 | 0.14 |
| 190 | 7.66 | 0.69 | 0.38 | 0.13 |
| 190 | 7.55 | 0.74 | 0.35 | — |
| 190 | 7.74 | 0.68 | 0.36 | — |

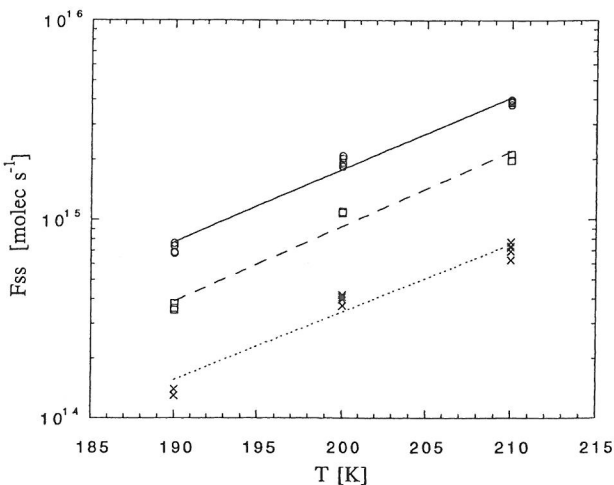


Fig. 4

Observed steady state levels of HCl in the aftermath of a pulse in terms of absolute flow effusing out of the Knudsen cell as a function of temperature using the 15 mm (solid line), 8 mm (dashed line) and 4 mm orifice (dotted line)

correlated to the frequency of injection. In fact, it is only at high frequency that the HCl signal in between each pulse has approximately the same amplitude (top of Fig. 3) compared to the one obtained after a single large dose has been dispensed thus leading to the steady state displayed at the right hand corner of Fig. 3.

Several observations may be mentioned, keeping in mind that each experiment has been performed on a new ice sample:

- 1) A steady state level of HCl is only observable when the injected dose exceeds a threshold value. The mini-

Table 3

Mean values of the rate constant of adsorption (k_{eff}) and uptake coefficient γ on fresh ice as a function of temperature obtained by fitting the time-dependent MS signal to an exponential decay function. The middle column displays the threshold dose for the temperature of interest

| Low doses | | Dose threshold | High doses | |
|-----------|------------------------------|----------------|--|------------------------------|
| T [K] | k_{eff} [s ⁻¹] | γ | [molec cm ⁻²] 10^{13} | k_{eff} [s ⁻¹] |
| 190 | 31±2 | 0.34 | 6.7±0.5 | 28±2 |
| 200 | 26±2 | 0.26 | 20.0±5.0 | 18±2 |
| 210 | 20±2 | 0.22 | 27.0±5.0 | 12±2 |

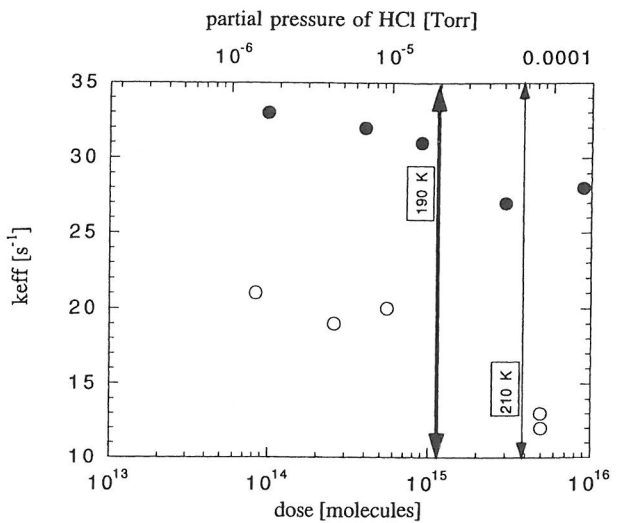


Fig. 5

Plot of k_{eff} as a function of dose at $T=190$ K (full circles) and 210 K (open circles). The values displayed to the left of the vertical bold (full circles) and normal (open circles) solid arrow correspond to the rate of adsorption without formation of a steady state level at 190 and 210 K, respectively. The value of k_{eff} to the right was measured in experiments at doses larger than the threshold limit which led to a steady state level. The position of the threshold level represented by the vertical double arrows was obtained in high frequency RPE's, as explained in the text

mum dose which still leads to an observable steady state HCl signal is referred to as the dose threshold.

- 2) The steady state level of HCl in a single pulse experiment such as displayed in Fig. 2 is constant regardless of the chosen HCl dose and only depends on the temperature and the orifice size, irrespective of the HCl density in the reactor (Table 2 and Fig. 4). The steady state persists for a given amount of time, depending on the injected dose, and gradually vanishes to zero after the supply of HCl from the surface is waning.
- 3) A steady state level is also observed in RPE experiments (upper trace in Fig. 3). However, the dependence of the steady state HCl signal in between each pulse of the RPE suggests the possibility of loss by diffusion from the surface to the bulk. With decreasing repetition frequency the adsorbed HCl has sufficient

time in between pulses to diffuse into the bulk, most probably along cracks, grain boundaries or other crystal imperfections. This would explain the decreasing HCl steady state level with decreasing repetition frequency (Fig. 3, going from top to bottom).

- 4) The numerical value of the dose threshold is estimated from RPE's at high frequency (upper trace in Fig. 3) by multiplying the number of pulses necessary to reach the steady state level with the dose of the individual pulse retained by the ice. This threshold varies from $1 \cdot 10^{15}$ to $4 \cdot 10^{15}$ molecules of HCl over the temperature range 190 to 210 K, corresponding to $6.7 \cdot 10^{13}$ to $2.7 \cdot 10^{14}$ molecules of HCl cm^{-2} (middle column in Table 3 and arrows in Fig. 5), thus between 10 and 45% of a formal monolayer of HCl.
- 5) The kinetics of HCl adsorption on a fresh ice sample depends on the injected dose. In single shot experiments performed at low doses, the rate of adsorption k_{eff} has been observed to be always higher than in experiments performed at large doses (Tables 3 and 4). At low dose, the value of k_{eff} is determined by fitting the decay of the reactive pulse according to a single exponential function followed by subtracting the escape rate constant k_{esc} from the total decay constant k_{dec} (Eq. (1)). In pulsed valve experiments performed at doses leading to the formation of a steady state level, k_{eff} is determined by fitting the initial time-dependent portion of the pulse relative to the steady state level and subsequently correcting for k_{esc} , as above.
- 6) In the dose range to both sides of the dose threshold, we did not find any dependence of k_{eff} on the dose in the range 10^{14} to 10^{16} molecules and on the gas residence time, thus confirming that the interaction of HCl on ice is a first order process.

Interpretation of Pulsed Valve Experiments

As far as the pulsed valve experiments are concerned, we have two experimental observables, namely the steady state HCl levels characteristic of a certain orifice and temperature, as well as k_{eff} corresponding to the single exponential decay of the transient HCl signal, either to background in the case of sub-threshold doses, or to a steady state level for doses exceeding the dose threshold (Figs. 2 and 3).

Detailed balancing leads to the following equation using a simple mechanism in which HCl in the gas phase (HCl_g) and in the adsorbed state (HCl_{ads}) are connected by the adsorption rate constant k_{ads} and the rate of desorption, R_{des} [30]:

$$\frac{d}{dt} [\text{HCl}]_g = -k_{\text{esc}} \cdot [\text{HCl}]_g - k_{\text{ads}} \cdot [\text{HCl}]_g + R_{\text{des}} \quad (2)$$

Eq. (2) may be expressed for desorption of HCl at steady state conditions in the aftermath of a large HCl pulse by taking into account the relation $\frac{F_{\text{SS}}}{V} = R_{\text{SS}} = k_{\text{esc}}[\text{HCl}]_g$:

Table 4

k_{eff} measured as a function of dose using the 15 mm diameter escape aperture; the values of k_{eff} measured at low doses are larger than the ones at higher doses. The values of k_{uni} , obtained in steady-state experiments and displayed in the right hand column, are to be compared to the values of k_{eff} measured in pulsed experiments at low doses. Typical low HCl flows of $3 \cdot 10^{14}$ molecule s^{-1} were used

| T [K] | Dose [molec] 10(15) | k_{eff} [s^{-1}] | k_{uni} [s^{-1}] |
|-------|------------------------|--------------------------------------|--------------------------------------|
| 210 | 0.55 | 21.0 | 15.0 |
| 210 | 0.53 | 19.5 | 16.0 |
| 210 | 0.55 | 19.5 | 15.5 |
| 210 | 5.36 | 13.0 | |
| 210 | 5.10 | 11.4 | |
| 210 | 5.18 | 13.8 | |
| 210 | 5.16 | 13.9 | |
| 200 | 0.97 | 26.6 | 20.1 |
| 200 | 0.98 | 26.2 | 17.9 |
| 200 | 0.97 | 24.6 | 22.3 |
| 200 | 9.38 | 16.8 | |
| 200 | 9.16 | 20.0 | |
| 200 | 9.18 | 18.5 | |
| 190 | 0.87 | 30.2 | 32.0 |
| 190 | 0.86 | 30.1 | 29.0 |
| 190 | 0.87 | 33.3 | 26.0 |
| 190 | 7.92 | 29.5 | |
| 190 | 7.66 | 28.4 | |
| 190 | 7.55 | 27.0 | |
| 190 | 7.74 | 27.0 | |

$$-F_{\text{SS}} - k_{\text{ads}} \cdot \frac{F_{\text{SS}}}{k_{\text{esc}}} + F_{\text{des}} = 0 \quad (3)$$

F_{SS} is the flow of HCl in molecule s^{-1} leaving the reactor and is thus proportional to the MS signal of HCl monitored at m/e 36. F_{SS} stays constant on the experimental time scale of a few seconds which is long compared to the decay of the MS transient which leads to the establishment of a steady state on the time scale of 0.1 to 0.3 s. The steady state signal levels displayed in Fig. 2 result from the balance between the rate of HCl adsorption, the rate of desorption of HCl from the sample, F_{des} , and the rate of escape of HCl out of the Knudsen cell, F_{SS} . The steady state therefore corresponds to an equilibrium between the rate of adsorption and desorption perturbed to a variable extent by the escape rate of HCl. We will show in the next paragraph how to calculate the equilibrium vapor pressure starting from the kinetics (k_{eff} given in Tables 3 and 4) and the steady state vapor pressure (given by F_{SS} in Table 2) measured in the aftermath of a HCl pulse.

Activation Energy and Thermochemistry

In order to separate the two kinetic parameters k_{ads} and R_{des} , we assume that the single exponential decay constant obtained in pulsed valve experiments is identical to the adsorption rate constant k_{ads} , leading to $k_{\text{ads}} \equiv k_{\text{eff}}$.

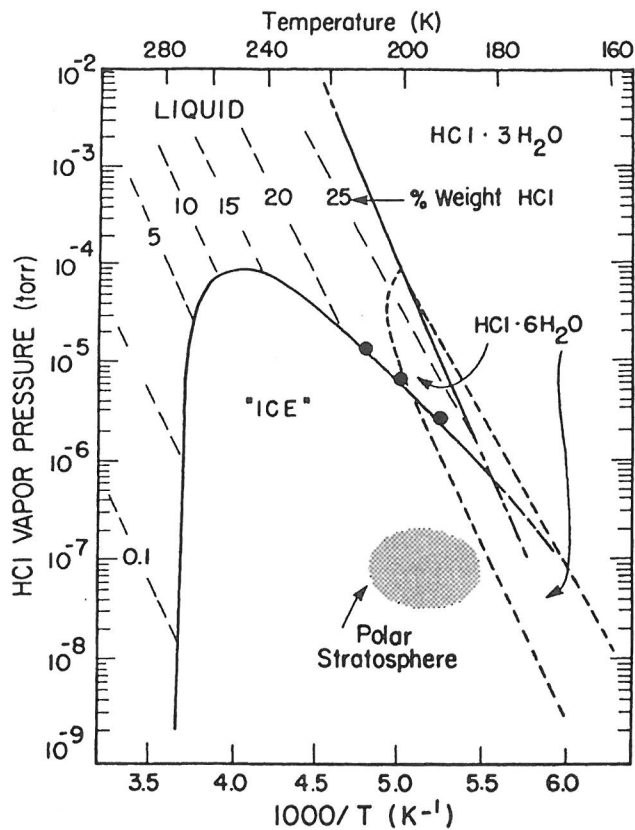


Fig. 6

Phase diagram of the HCl/H₂O system constructed by Molina and coworkers [24]. The full circles on the “ice”/liquid coexistence line represent calculated values using the kinetic data for adsorption and desorption from pulsed valve experiments of the present work

Following Eq. (3) the relationship between equilibrium and the observed steady state rate of desorption of HCl from ice is given in Eq. (4):

$$F_{\text{des}} = F_{\text{ss}} \left(1 + \frac{k_{\text{eff}}}{k_{\text{esc}}} \right) \quad (4)$$

The equilibrium vapor pressure may now be calculated:

$$P_{\text{eq}} = \left(\frac{R_{\text{des}}}{k_{\text{ads}}} \right) RT = \left(\frac{F_{\text{des}}}{k_{\text{eff}} \cdot V} \right) RT \quad (5)$$

where F_{des} is the rate of desorption in molecule s⁻¹ calculated from the measured steady state value F_{ss} .

In this way we have separately determined k_{eff} , thus k_{ads} and F_{des} within a single pulsed valve experiment in which the HCl/ice sample reached steady state. Our assumption cited above, $k_{\text{ads}} = k_{\text{eff}}$, is equivalent to the statement that the pulse decay corresponds to the rate of adsorption, characterized by k_{eff} with respect to a constant desorption rate established during the valve opening time or shortly thereafter. This is supported by the fact that k_{eff} follows a first order rate law for a variation of the HCl dose over three orders of magnitude. More specifically, a typical dose of 10¹⁶ molecules of HCl per pulse

Table 5

Value of the rate of desorption R_{des} and equilibrium vapor pressure as a function of temperature obtained in pulsed valve experiments

| T [K] | Rate of desorption R_{des} 10(12) molec s ⁻¹ cm ⁻³ | HCl vapor pressure 10(-5) Torr |
|---------|--|-----------------------------------|
| 210 | 9.98 | 1.44 |
| 210 | 10.30 | 1.48 |
| 210 | 10.22 | 1.48 |
| 200 | 6.62 | 0.74 |
| 200 | 6.32 | 0.82 |
| 200 | 6.03 | 0.82 |
| 190 | 2.90 | 0.31 |
| 190 | 2.62 | 0.28 |
| 190 | 2.81 | 0.30 |
| 190 | 2.59 | 0.28 |

leads to a deposition rate of half of a monolayer of HCl per millisecond at an uptake coefficient of 0.5. This shows that the chosen experimental conditions are consistent with the assumption of a rapid establishment of steady state conditions on the ice sample once a sufficiently large HCl pulse has been admitted. In practice, the decay of the HCl signal is observed after some 20 ms after admission of the HCl pulse because of the limitation imposed by molecular flow and because of the limited instrument rise time [31].

The values obtained for the HCl equilibrium vapor pressure from our kinetic measurements (full circles in Fig. 6, Table 5) coincide within experimental error with the vapor pressure at the coexistence curve for HCl solutions and their corresponding solid in the phase diagram of the H₂O/HCl system measured at equilibrium by Molina and co-workers [4, 8, 32, 33]. We therefore conclude that the observed steady state level in the aftermath of pulsed dosing experiments at doses exceeding the dose threshold does in fact originate from the desorption of HCl from a concentrated solution of HCl formed on the ms time scale after injection of the pulse.

The formation of the HCl solution is supported by the fact that the duration of the steady state level is proportional to the number of molecules of HCl injected. Under these conditions variable amounts of HCl are dissolved in ice by surface melting resulting in a concentrated liquid solution of HCl in ice owing to the large exothermicity of the process [4]. This solution gives rise to a constant rate of desorption which depends only on temperature regardless of the quantity of the liquid solution, provided there is homogeneous coverage of HCl on ice. In Knudsen cell studies of heterogeneous reactions all surface elements of the condensed phase have been exposed to the same amount of gas. As a consequence there are now three phases in the system: solid ice which may contain traces of HCl, a liquid HCl/H₂O mixture, in which the HCl is electrolytically dissociated and the gas phase.

In case of a HCl dose below threshold (lowest trace in Fig. 2) we do not observe a constant release of HCl after a pulse, thus there is no observable rate of desorption.

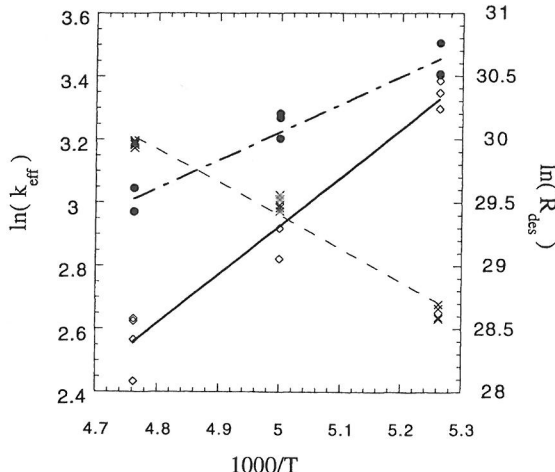


Fig. 7

Arrhenius representation of the rate of desorption R_{des} and the rate constants $k_{\text{ads}} = k_{\text{eff}}$. a) The dashed line with crosses (right hand ordinate) represents the net rate of desorption calculated from the data obtained in pulsed valve experiments using the 15 mm diameter orifice (Table 5). b) The two other lines are linear fits of k_{eff} (left hand ordinate) determined in pulsed valve experiments; the upper (dot-dashed) line with full circles is obtained using k_{eff} pertaining to small individual pulses without observation of the steady state level, the solid line with open square symbols corresponds to a large dose leading to a true liquid state

The interaction of HCl on ice is therefore dominated solely by adsorption as well as by diffusion on the surface and into the bulk, probably along dislocations, defects and cracks. The state of the $\text{H}_2\text{O}/\text{HCl}$ interface giving rise to a partial pressure lower than the HCl equilibrium vapor pressure or no observable vapor pressure is said to be a quasi-liquid state or solid solution of HCl in ice. The occurrence of the HCl equilibrium vapor pressure is therefore a discriminating criterion for the state of the HCl/ice interface, as has been pointed out in the literature [34].

An Arrhenius plot of k_{eff} in the temperature range 190 to 210 K shows a negative activation energy $E_{\text{a}1}$ equal to -1.8 ± 0.3 kcal/mol for experiments at low doses of typically $5 \cdot 10^{14}$ molecules per pulse leading to a quasi-liquid state of HCl on ice. $E_{\text{a}2}$ was determined to be -3.1 ± 0.3 kcal/mol for experiments at high doses of typically $5 \cdot 10^{15}$ molecules per pulse leading to surface melting and resulting in a liquid solution of HCl in ice (Fig. 7). Both negative values suggest a complex mechanism implying a precursor state. From these results, it is apparent that the uptake process of HCl on ice in the presence of a transient supersaturated partial pressure of HCl falls into two categories: the “dry” adsorption/desorption process of HCl leading to a quasi-liquid state of the $\text{HCl}/\text{H}_2\text{O}$ interface (full circles in Fig. 7) is always faster than the process leading to the “wet” system, that is a liquid $\text{HCl}/\text{H}_2\text{O}$ mixture after surface melting (open diamonds and crosses in Fig. 7). The HCl desorption rate from the liquid given by the crosses in Fig. 7 exponentially increases with temperature and leads to a positive activation energy E_{des} of 5.0 ± 1 kcal/mol leading to an enthalpy change of

8.1 ± 1.3 kcal/mol. It has to be noted, however, that this enthalpy does not correspond to an elementary process, such as the phase change of HCl from the condensed to the gas phase, because the composition of the condensed phase is not held constant as the temperature is changed. The solid-liquid coexistence line is the “end point” of many different vapor pressure vs. inverse temperature curves following the relation of Clausius-Clapeyron, some of which are displayed in Fig. 6 as the dashed straight-lines labeled “% weight HCl”. Fig. 7 also shows that the linear fits to k_{eff} obtained in the pulsed valve experiments corresponding to the “dry” and the “wet” adsorption/desorption process seem to converge to a common value of 185 ± 1 K, a characteristic value which may be found in the $\text{HCl}/\text{H}_2\text{O}$ phase diagram. This result indicates that this temperature is the lowest at which a liquid can coexist with its gaseous phase and may thus be interpreted as an eutectic point [26].

Repetitive Pulse Experiments (RPE)-Surface Loss by Diffusion

Does the repeated injection of small doses of HCl in RPE’s, with each individual dose insufficient to lead to liquid $\text{HCl}/\text{H}_2\text{O}$ mixtures, give rise to the formation of a liquid layer by accumulation, like in the previously discussed single pulsed valve experiments? We will discuss the RPE experiment, as displayed in Fig. 3 in more detail. The MS signal of the first pulse on a fresh ice sample in the high frequency series (3.5 Hz, upper trace) exponentially decreases to its initial background level. From the fifth or sixth pulse onwards at approximately $t=2$ s, a steady state level of the HCl MS signal is observed which persists if the surface is charged continuously with additional pulses of HCl. At this point, the height of the steady state MS signal in between pulses is identical to that obtained in experiments performed at a single pulse of comparative cumulative dose such as displayed at the right hand corner of Fig. 3. When the injection frequency decreases to 1.66 Hz (middle trace of Fig. 3), a steady state level of the HCl signal is obtained after approximately 4 s. Its magnitude, however, is only half that of the one obtained in the high frequency series. In the lowest trace of Fig. 3 corresponding to an injection frequency of 0.91 Hz, no steady state HCl signal is observable within experimental uncertainty. This experiment at low but often repeated exposure then shows that even a dose below threshold may lead to a steady state HCl signal if the pulses are repeated at a sufficiently high frequency, whereas the same dose applied at a lower frequency will not lead to as high a steady state or no HCl signal (Fig. 3, lowest trace).

This result suggests the possibility of loss from the surface into the bulk. We will show how to determine this loss rate from a series of pairs of RPE’s, where we inject a given fixed individual dose per pulse, once at higher frequency (f_1) for a shorter time (t_1) and then at lower frequency (f_2) for a longer time (t_2). Typically, the chosen

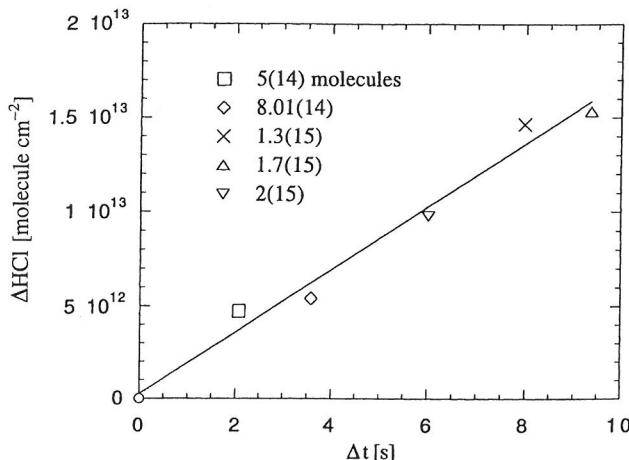


Fig. 8

Evaluation of the surface loss at $T=200$ K. The individual dose is $1.5 \cdot 10^{14}$ molecules per pulse. The difference of HCl molecules lost to the bulk in a pair of two RPE's is displayed as a function of the additional time ($\Delta t = t_2 - t_1$) necessary for the low frequency RPE to expose the ice surface to the same amount of HCl as the high frequency RPE. The corresponding rate of loss is determined from the slope of the best least-squares line and is $1.7 \cdot 10^{12}$ molecule $s^{-1} \text{cm}^{-2}$. The different symbols represent the total cumulative dose of HCl molecules injected into the reactor

frequency was in the range between 3.5 and 0.5 Hz. For a given total injected dose, where $t_1 f_1 = t_2 f_2$, the total fraction of HCl molecules released back into the gas phase decreased with decreasing frequency of injection. The reason for this is simply that the HCl molecules have more time to disappear at low frequency between pulses from the surface into the bulk than at high frequency. The difference of HCl molecules lost to the bulk, and thus non-retrievable, in a pair of two RPE's is therefore a function of the additional time ($\Delta t = t_2 - t_1$), necessary for the low frequency RPE to expose the ice surface to the same amount of HCl as the high frequency RPE. As illustrated graphically in Fig. 8, a plot of ΔHCl versus Δt results in a straight line, demonstrating that the rate of surface-to-bulk loss (given by the slope) remains constant over the range of total injected doses. The rate of surface-to-bulk determined in this example results in a value of $1.7 \cdot 10^{12}$ molecule $s^{-1} \text{cm}^{-2}$. In order to prevent any misunderstanding, we will emphasize that this is not a measurement of the Fickian diffusion coefficient, but rather a competitive loss or dissipation process preventing the desorption of HCl once it is adsorbed on the ice surface.

The results obtained according to the above description are independent of the pair of injection frequencies, in the range from 0.3 to 3.5 Hz (the fastest that we can obtain with our apparatus) within experimental error. As a result the rate of surface-to-bulk disappearance seems to be independent of the given initial HCl partial pressure in each RPE of a given pair. We investigated this process also by varying the individual dose in the range 10^{14} to $5 \cdot 10^{15}$ HCl molecules per pulse. Fig. 9 displays the rate of surface-to-bulk loss ranging from 10^{12} to 10^{13} molecule $s^{-1} \text{cm}^{-2}$, calculated as above and found to be independent of

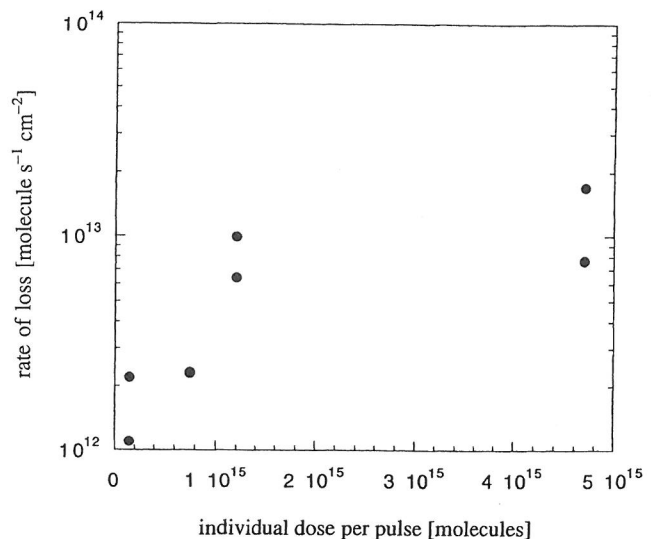


Fig. 9

Calculated rate of surface-to-bulk loss as a function of the individual dose in RPE's at 200 K. Each point is calculated as explained in the text, using a pair of RPE's with an example in Fig. 8

Table 6

Comparison of the rate of adsorption and surface loss. The deposition rate corresponding to stratospheric conditions in the third column are calculated at ^a) $P_{\text{HCl}} = 10^{-7}$ Torr and ^b) $P_{\text{HCl}} = 10^{-8}$ Torr. The experimental rate of adsorption in the fourth column is calculated as $k_{\text{eff}} \cdot \text{dose}$, with a dose of 5(14) molecules in the example

| Rate of adsorption [molecule $s^{-1} \text{cm}^{-2}$] | | | |
|--|--------------|-------------------------|---|
| T [K] | Experimental | Stratosphere | Surface loss [molecule $s^{-1} \text{cm}^{-2}$] |
| 190 | 1(15) | $4.2(13)^a$ $4.2(12)^b$ | $< 1.3(12)$ |
| 200 | 8.7(14) | $4.1(13)^a$ $4.1(12)^b$ | $1.3 \pm 0.1(12)$ |
| 210 | 6.7(14) | $4.0(13)^a$ $4.0(12)^b$ | $2.6 \pm 0.1(12)$ |

the pair of injection frequencies. These results suggest that the rate of surface-to-bulk loss is zero order in HCl for pulses exceeding 10^{15} molecules per pulse, that is when the HCl/ice system is in the liquid state. At this point the loss rate of HCl into bulk ice apparently becomes independent of the surface concentration of adsorbed HCl. In summary, if there was no surface-to-bulk loss, the number of molecules lost at the surface would be the same for both pulse series (f_1, f_2) and would not depend on the frequency of the injection. However, the longer the elapsed time between pulses, the more pronounced was the measured loss of HCl thus preventing desorption.

Table 6 displays the rate of surface-to-bulk loss (fourth column) in units of molecule $s^{-1} \text{cm}^{-2}$. In comparison, the rate of adsorption expressed in the same units are shown in the third column. We conclude that the rate of surface loss is actually more or less 1% of the rate of adsorption for the temperature range 190 to 210 K and may therefore be neglected in our experiments [18]. However, the deposition rate of HCl at stratospheric conditions (third

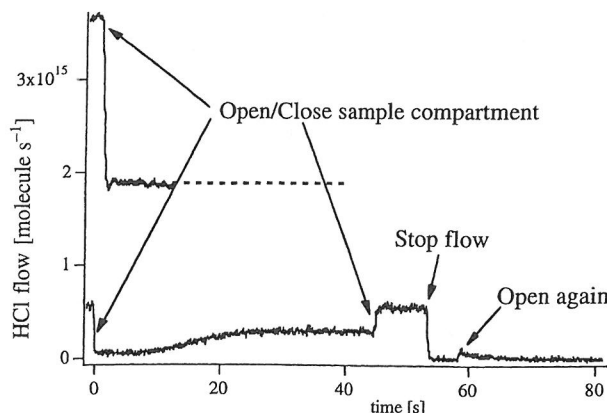


Fig. 10

Typical steady state experiments at low ($6 \cdot 10^{14}$ molecule s^{-1}) and high flow rate ($3.6 \cdot 10^{15}$ molecule s^{-1}) of HCl at 185 K, respectively. For a flow of $3.6 \cdot 10^{15}$ molecule s^{-1} , the initial steady state is not observed due to rapid saturation

column in Table 6) is of the same order of magnitude as the rate of surface-to-bulk diffusion determined in our experiments. We therefore point out a possible consequence of a significant rate of dissipation under stratospheric conditions where the concentration of HCl is smaller than in our experiment (10^{-7} to 10^{-6} Torr) but where the time scales are also much longer (on the order of days to months). In this way, even admitting a lower rate of surface-to-bulk diffusion in type II PSC's, a sufficient amount of HCl could diffuse from the surface of the ice crystals into the bulk thus preventing HCl accumulation at the surface and subsequent heterogeneous reaction.

Furthermore, the rate of HCl adsorption gradually decreases when several small pulses are introduced to the same ice sample. The rate of "dry" adsorption of HCl leading to the quasi-liquid state drops from 31, 26 and 20 ± 2 s^{-1} (fresh ice) to 28, 18, 12 ± 2 s^{-1} once several pulses have been injected at 190, 200 and 210 K, respectively (Table 3). The values of k_{eff} for dry adsorption on an aged, that is previously exposed, surface are equal to those for the adsorption of HCl leading to a liquid solution of HCl/H₂O, corresponding to the "wet" adsorption process. Therefore the rates of the "dry" and "wet" adsorption processes are identical on an aged sample, suggesting a memory effect. In addition, an ice sample once exposed to HCl preserves its adsorption properties of lower values of k_{eff} even after prolonged pumping at 10^{-5} Torr, thus demonstrating the memory effect by contamination.

Steady State Experiments

Support of the results obtained in pulsed valve experiments.

Steady state experiments were performed at HCl partial pressures in the range between $5 \cdot 10^{-7}$ and $2 \cdot 10^{-4}$ Torr calculated according to $P_{\text{HCl}} = (F_i/k_{\text{esc}} V)RT$. Fig. 10

shows two typical steady state experiments, one at a low flow of HCl ($F_i = 5.6 \cdot 10^{14}$ molecule s^{-1} , $T = 185$ K, 15 mm orifice) and another at a high flow ($F_i = 3.6 \cdot 10^{15}$ molecule s^{-1} , $T = 200$ K, 8 mm orifice). At low HCl flow, we observe the uptake of HCl leading to the formation of a low steady state level for a few seconds. A second higher steady-state level F_{ss} is established corresponding to a lower net uptake rate at $t = 25$ s at the conditions of Fig. 10 as a consequence of a partial saturation process. At a high flow rate of HCl, we observe only one steady state level. The second steady state level under low flow conditions and the single steady state at high flow persist for the whole duration of the experiment up to a few minutes whereas the duration of the first steady state level (low flow) depends on the partial pressure of HCl. After we lowered the plunger thus isolating the sample, we halted the flow, lifted the plunger again and observed a small amount of HCl released into the gas phase. This is a measure of the retrievable fraction of HCl and will be discussed below as a function of the temperature and flow rate of HCl.

It is important to note that the uptake kinetics strongly depends on the history of the sample: when successive experiments on the same sample are performed, the initial uptake on the increasingly aged sample is always smaller than the former, even when we allow a large fraction of the adsorbed HCl to be released into the gas phase after the previous experiment by pumping on the sample. This result is in agreement with the observation of a memory effect discussed above concerning the pulsed valve experiments. Thus the HCl-ice interaction presents some aspect of irreversibility, which is also confirmed in steady state experiments.

The value of the initial first order uptake rate constant on a fresh ice sample, namely $k_{\text{uni}} = (F_i/F_{\text{ss}} - 1) \cdot k_{\text{esc}}$, confirms the value of k_{eff} obtained in pulsed valve experiments performed at low doses for each temperature (see Table 4 comparing columns 3 and 4). We assume that the rate of desorption is vanishing during the initial steady state level at low flow (displayed in Fig. 10). Eq. (2) is expressed for steady state conditions in Eq. (6):

$$V \cdot \frac{d}{dt} [\text{HCl}]_g \Big|_{\text{ss}} = -F_{\text{ss}} - k_{\text{ads}} \cdot \frac{F_{\text{ss}}}{k_{\text{esc}}} + F_{\text{des}} + F_{\text{HCl}}^i = 0 \quad (6)$$

As k_{uni} equals k_{eff} , which we have assumed to be equal to k_{ads} in Eqs. (2) and (3), Eq. (6) implies that F_{des} is vanishing during the initial steady state (F_{ss}).

After $(1.0 \pm 0.2) \cdot 10^{15}$ HCl molecules have been taken up at ~~200~~ K, the desorption rate F_{des} becomes competitive with adsorption and escape at $t = 15$ s for the lower trace in Fig. 10 so that the surface tends towards steady state corresponding to the onset of the second steady state level. At this point $(5 \pm 2) \cdot 10^{15}$ molecules have been adsorbed onto the 15 cm^2 ice sample, which is consistent with the threshold value given in Table 3. In summary, steady state

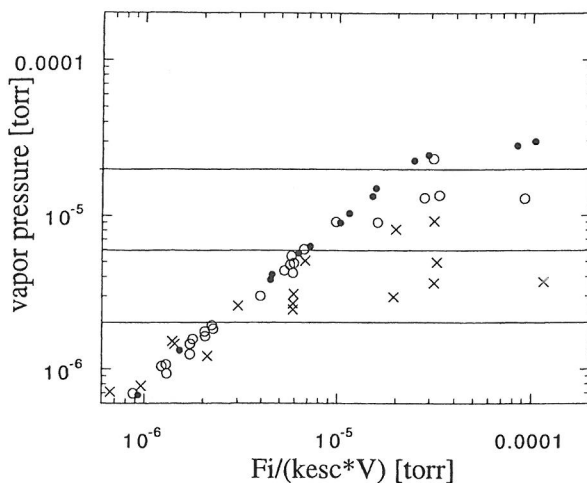


Fig. 11

Plot of the calculated equilibrium vapor pressure at 190, 200 and 210 K as a function of the initial partial pressure P_{HCl} in the reactor defined as $F^i/(k_{\text{esc}} V)$, represented by crosses, open circles and full circles, respectively. F^i is the flow of HCl into the reactor, k_{esc} the rate of effusion out of the Knudsen cell whose volume is V . The solid lines are the values of the vapor pressure from the work of Molina and coworkers

experiments show the heterogeneous interaction and the resulting state of the interface in two phases: the initial uptake of HCl on fresh ice leads to the first steady state level given only by the kinetics of adsorption. After a given amount of HCl has been adsorbed there is formation of a HCl/H₂O mixture sustaining an equilibrium between adsorption and desorption and the rate of escape. The partial pressure of HCl controls the rate at which the system reaches the perturbed adsorption/desorption equilibrium: at high flow rate, the steady state between adsorption, desorption and rate of escape is reached already at the beginning of the experiment.

The rate of desorption corresponding to the second steady state level of HCl was calculated using the following expression derived from Eq. (6) for steady state conditions:

$$F_{\text{des}} = F_{\text{SS}} \left(1 + \frac{k_{\text{eff}}}{k_{\text{esc}}} \right) - F_{\text{HCl}}^i \quad (7)$$

It leads to the expression for the equilibrium vapor pressure of HCl:

$$P_{\text{eq}} = \frac{R_{\text{des}}}{k_{\text{ads}}} RT = \frac{F_{\text{SS}} \left(\frac{k_{\text{eff}}}{k_{\text{esc}}} + 1 \right) - F_{\text{HCl}}^i}{V k_{\text{eff}}} RT \quad (8)$$

Although we measure HCl partial pressures under steady state or transient conditions, the sample surface is in thermodynamic equilibrium with its gas phase, albeit perturbed by k_{esc} owing to the fact that the present experiments are performed in a flowing gas experiment. The measured HCl partial pressures lead to values of k_{ads} and

Table 7

Rate of desorption and calculated equilibrium vapor pressure of HCl as a function of the initial partial pressure in the reactor expressed as $F^i/(k_{\text{esc}} \cdot V)$ obtained in steady state experiments. It was calculated using the second steady state level ($F_{\text{SS}}(\text{HCl})$) such as displayed in Fig. 10 and the value of k_{eff} in Eq. (6) for k_{ads}

| T [K] | Initial pressure of HCl $10(-5)$ Torr | Rate of desorption R_{des} [molecule s ⁻¹ cm ⁻³] | Equilibrium vapor pressure $10(-5)$ Torr |
|---------|---|--|--|
| 210 | 0.15 | 0.84 | 0.13 |
| | 0.44 | 2.44 | 0.38 |
| | 0.45 | 2.64 | 0.41 |
| | 0.63 | 3.64 | 0.56 |
| | 0.73 | 4.03 | 0.63 |
| | 1.03 | 5.73 | 0.89 |
| | 1.14 | 6.61 | 1.03 |
| | 1.5 | 9.59 | 1.49 |
| | 1.51 | 8.52 | 1.33 |
| | 2.46 | 14.41 | 2.25 |
| | 2.91 | 15.64 | 2.44 |
| | 8.41 | 18.06 | 2.82 |
| | 10.3 | 19.19 | 2.99 |
| | 0.08 | 0.57 | 0.06 |
| | 0.12 | 0.87 | 0.10 |
| | 0.12 | 0.89 | 0.10 |
| | 0.13 | 0.77 | 0.09 |
| | 0.17 | 1.03 | 0.12 |
| | 0.17 | 1.21 | 0.14 |
| | 0.17 | 1.29 | 0.15 |
| | 0.20 | 1.35 | 0.16 |
| | 0.20 | 1.45 | 0.17 |
| | 0.22 | 1.52 | 0.18 |
| | 0.22 | 1.60 | 0.19 |
| | 0.39 | 2.49 | 0.30 |
| | 0.57 | 3.65 | 0.43 |
| | 0.56 | 3.98 | 0.47 |
| | 0.57 | 4.55 | 0.54 |
| | 0.58 | 3.51 | 0.42 |
| | 0.59 | 4.08 | 0.49 |
| | 0.66 | 5.02 | 0.60 |
| | 0.98 | 7.55 | 0.90 |
| | 1.60 | 7.51 | 0.90 |
| | 2.79 | 10.85 | 1.30 |
| | 3.09 | 19.27 | 2.31 |
| | 3.32 | 11.25 | 1.35 |
| | 9.21 | 10.68 | 1.28 |
| 190 | 0.03 | 3.41 | 0.34 |
| | 0.06 | 5.63 | 0.56 |
| | 0.07 | 0.70 | 0.07 |
| | 0.09 | 0.77 | 0.07 |
| | 0.14 | 1.44 | 0.14 |
| | 0.14 | 1.50 | 0.15 |
| | 0.21 | 1.20 | 0.12 |
| | 0.30 | 2.56 | 0.25 |
| | 0.67 | 5.05 | 0.51 |
| | 1.94 | 2.91 | 0.90 |
| | 1.99 | 8.06 | 0.81 |
| | 11.51 | 3.67 | 0.37 |

F_{des} which define the equilibrium in a closed system according to $[\text{HCl}]_{\text{eq}} = F_{\text{des}} / k_{\text{ads}} V$.

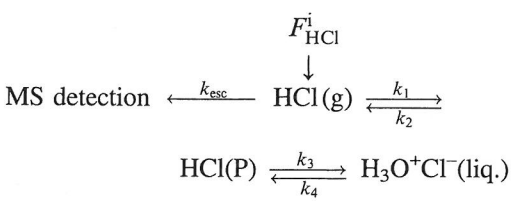
Fig. 11 and Table 7 present values of the calculated equilibrium HCl vapor pressure computed from the observed steady state values of F_{SS} corresponding to the

second steady state level at low flow (lower trace in Fig. 10) and the kinetics of adsorption (k_{eff} from Table 4) as a function of the experimental initial concentration of HCl expressed as $(F_i/k_{\text{esc}} \cdot V)RT$. We note that the calculated equilibrium vapor pressure strongly depends on the initial flow of HCl. In fact, the equilibrium vapor pressure, determined at high doses in pulsed valve experiments and found in agreement with the literature [2, 8], is obtained when the partial pressure of HCl in the reactor is high enough to lead to the formation of a liquid HCl/H₂O mixture. We admit that the values corresponding to the asymptotes of the steady state vapor pressure are larger by a factor of two in relation to those calculated using pulsed valve experiments.

We point out that the kinetic results from steady state experiments at low flow rates characterized by the value of k_{uni} at the initial steady state level (fourth column in Table 4) corresponds to a quasi-liquid or solid solution of HCl on ice identical to that obtained after a single pulsed valve experiment performed at low dose where the rate of desorption is not observable (third column in Table 4, low dose). The quasi-liquid and liquid nature of the HCl/ice surface are thus revealed both in pulsed valve and steady state experiments as a function of the frequency of RPE's and the initial flow of HCl, respectively. When the dose in pulsed valve experiments is large enough, or the frequency of a RPE is high enough to lead to the formation of a steady state level F_{SS} (upper trace in Fig. 3), the sample is obviously in the same thermodynamic state compared to steady state experiments performed at high initial concentrations of HCl leading to the asymptotic values of the vapor pressure displayed in Fig. 11. At a low frequency RPE or at a low flow steady state experiment the state of the HCl/H₂O sample is in the quasi-liquid state. An equilibrium pressure, lower than the asymptotic value, can nevertheless be calculated in agreement with the HCl/H₂O phase diagram.

The Precursor Mechanism

The first order rate law for the uptake of HCl on ice taken together with its negative temperature dependence call for a complex mechanism. We propose a mechanism in Scheme I which is the simplest extension of the one presented in Eq. (2):



Scheme I

In Scheme I HCl(P) is a precursor state to either the liquid HCl/H₂O solution or the quasi-liquid state both represented as $\text{H}_3\text{O}^+\text{Cl}^-(\text{liq.})$. At the low temperature end

the rate limiting process for HCl disappearance is reaction 3 (k_3) which allows the system to build up the concentration of P at the interface. The process k_2 corresponding to the desorption of P only depends on temperature. Its low value prevents desorption after initial uptake of HCl and therefore leads to an uptake rate which reaches a maximum at low temperature and low coverage. Towards higher temperatures k_2 increases faster than k_3 because the former process involves a phase transition with a sizeable latent heat on the order of 5 kcal/mol (see R_{des} in Fig. 7). In addition, k_3 is expected to be independent of temperature because it corresponds to electrolytic dissociation. This relative increase of the ratio k_2/k_3 with increasing temperature may explain the increase of the desorption rate during the transient supersaturation experiment which is responsible for the apparent decrease of the net uptake coefficient with temperature. This increasing rate of desorption therefore originates from the desorption of the precursor P given by k_2 as long as its coverage on ice is significant.

The hallmark of the precursor mechanism given in Scheme I is the feature of competition between processes k_2 and k_3 which changes with temperature and the presence of two distinguishable species in the condensed phase, namely HCl(P) and $\text{H}_3\text{O}^+\text{Cl}^-(\text{liq.})$. This precursor mechanism is formally identical to the one proposed for H₂O(g) condensation on ice [35, 36] which however was later withdrawn by Brown et al. [37]. However, Scheme I is an oversimplification of the uptake kinetics because we have measured a first order rate constant for dissipation or surface-to-bulk diffusion which may compete for P but which has not been included in the mechanism. The presentation of a numerical model based on Scheme I will be presented elsewhere.

Retrievable Fraction of HCl

Steady state experiments allow us to characterize the reversibility of the interaction of HCl on ice, that is the fraction retrievable out of the bulk sample even after prolonged pumping. We define the retrievable fraction as the number of molecules of HCl desorbing from a previously exposed sample relative to the number of molecules adsorbed during the exposure of typically 50 s. We observed that this ratio does not depend on the duration of the HCl exposure to the surface. Fig. 12 shows the retrievable fraction expressed in percent at four temperatures of interest as a function of HCl flow and partial pressure. We observe that the retrievable fraction strongly depends on the state of the surface, either quasi-liquid or liquid HCl/H₂O mixture; when the partial pressure is below the vapor pressure at steady state conditions, that is when there is no formation of a liquid layer on the surface, the retrievable fraction is approximately only 10% at each temperature. This means that only 1 in 10 HCl molecules deposited may be retrieved at that temperature. When the sample forms a liquid HCl/H₂O mixture, the retrievable fraction becomes dependent upon temperature and is larger as

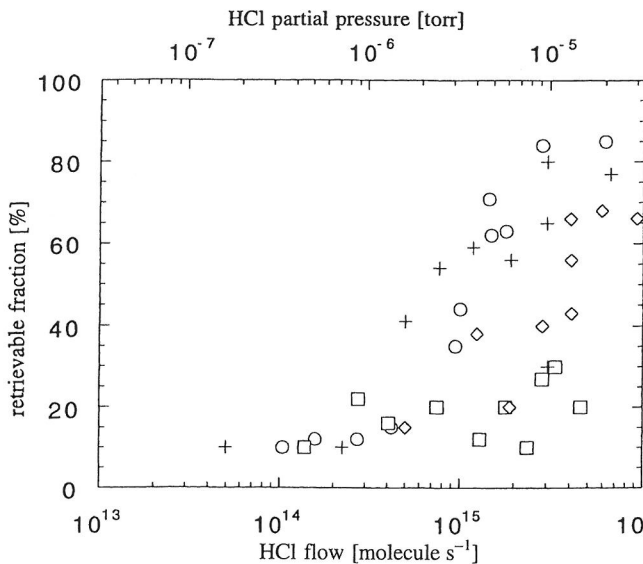


Fig. 12

Retrievable fraction expressed as percentage as a function of the partial pressure or flow of HCl at the temperatures of 180, 190, 200 and 210 K, represented by crosses, open circles, open diamonds and open squares, respectively. It is defined as the number of HCl molecules retrieved upon pumping at zero flow of HCl into the Knudsen cell relative to the total number of HCl molecules adsorbed in the previous uptake experiment

the temperature decreases (maximum is 80% at 180 K). This may be related to the diffusion process discussed above, whose rate increases with temperature: at high temperature more HCl will diffuse into the bulk of ice and is irretrievably lost, at least on the time scale of the present experiment, typically a few minutes.

The high rate of irreversible disappearance of HCl on the ice at low flow rates may be due to the diffusion of HCl molecules into the bulk along grain boundaries, defects and dislocations as noted by Wolff et al. [10]. When a liquid layer is formed on the surface at high flow rates, the liquid nature of the HCl/ice system leads to a lower temperature-dependent probability of dissipation.

Uptake of HBr and HI on Ice

We carried out pulsed valve and steady state experiments with HBr and HI on ice, prepared as described above. Both techniques, performed over the same range of dose and flow, only allowed us to measure the kinetics of adsorption. Table 8 shows the uptake coefficient γ of HCl, HBr and HI in the temperature range 190 to 210 K, determined in pulsed valve experiments. We obtained identical results in steady state experiments within experimental uncertainty. The kinetics of adsorption of HBr and HI is found to obey a first order rate law and has a negative temperature dependence (Fig. 13) indicating a complex mechanism analogous to Scheme I. Our results are in agreement with a recent study concerning the uptake of HBr on ice [38].

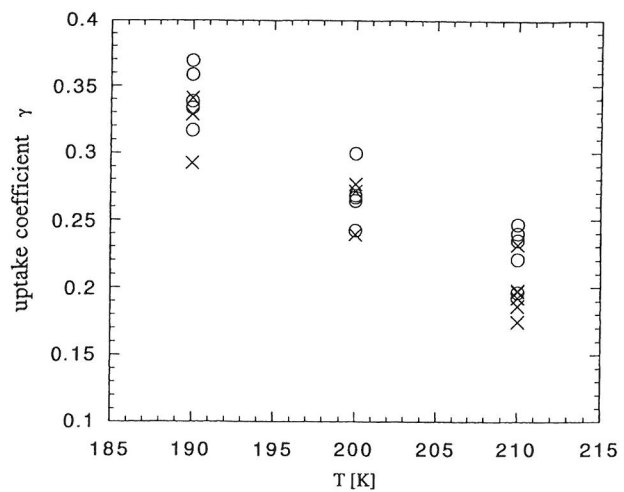


Fig. 13

Uptake coefficients γ of HBr (full circles) and HI (crosses) as a function of temperature, determined in pulsed valve experiments. The injected doses range from 10^{14} to 10^{16} molecules

Table 8

Uptake coefficients γ of HBr, HI and HCl as a function of temperature, determined from pulsed valve experiments. Each value corresponds to an uptake experiment carried out on a fresh ice sample. The doses of HBr and HI range from 10^{14} to 10^{16} molecules per pulse

| T [K] | HBr | HI | HCl ^a) | HCl ^b) |
|-------|------|------|--------------------|--------------------|
| 210 | 0.24 | 0.17 | 0.23 | 0.15 |
| 210 | 0.24 | 0.20 | 0.22 | 0.13 |
| 210 | 0.25 | 0.23 | 0.22 | 0.15 |
| 210 | 0.22 | 0.19 | | 0.16 |
| 210 | 0.20 | 0.19 | | |
| 210 | 0.22 | 0.20 | | |
| 200 | 0.30 | 0.24 | 0.30 | 0.19 |
| 200 | 0.24 | 0.27 | 0.29 | 0.22 |
| 200 | 0.27 | 0.28 | 0.27 | 0.21 |
| 200 | 0.27 | | | |
| 200 | 0.27 | | | |
| 190 | 0.34 | 0.29 | 0.34 | 0.33 |
| 190 | 0.33 | 0.34 | 0.34 | 0.32 |
| 190 | 0.32 | 0.33 | 0.37 | 0.30 |
| 190 | 0.34 | | | 0.30 |
| 190 | 0.32 | | | |
| 190 | 0.32 | | | |

^{a)} Uptake of HCl on the quasi-liquid layer

^{b)} Uptake of HCl on liquid HCl/H₂O solution

Contrary to the results on HCl, we did not observe a steady state level in the aftermath of large doses of HBr and HI expected to lead to an equilibrium between adsorption and desorption. In steady state experiments, the decrease of the signals monitored at m/e 80 and 128 for HBr and HI, respectively, results in a steady state level once the ice surface is exposed to the acid. This steady state remains stable during the whole duration of the experiment (typically on the order of minutes). In analogy to the observations made using pulsed valve experiments

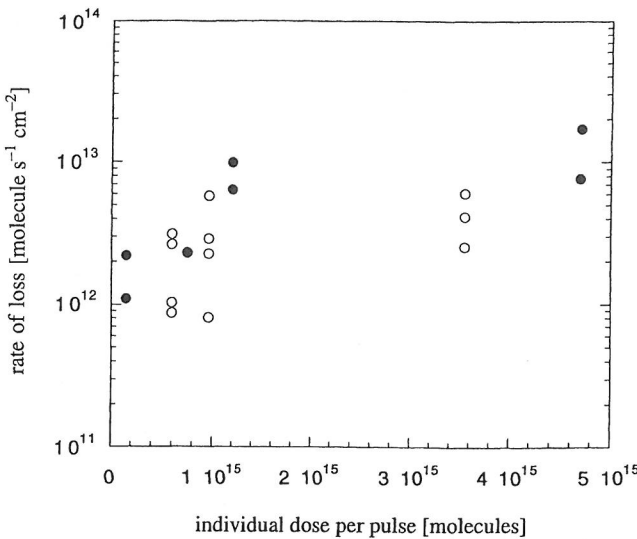


Fig. 14

Rate of surface-to-bulk loss of HBr (open circles) and HCl (full circles) at 200 K. Each point is calculated as explained in the text, using a pair of RPE's. The HBr loss is smaller by a factor two compared to the HCl loss

and the analysis of steady state experiments on the interaction of HCl with ice, we conclude that under our experimental conditions the heterogeneous interaction of HBr and HI on ice does not lead to a liquid solution and its associated vapor pressure. The high solubility of HBr and HI in ice may be the reason that we never observe any desorption of HBr and HI from the ice sample, like in the case of HCl. The adsorbed HX (X=Br, I) may therefore react with $n\text{H}_2\text{O}$ and give rise to the formation of stable hydrates, as suggested by Pickering [23].

In Fig. 14, we compare the rate of surface-to-bulk loss of HCl and HBr using RPE's at $T=200$ K. The values for HBr are a factor of two smaller than for HCl. This may not be surprising owing to the fact that the HBr diffusion coefficient in ice ($D=10^{-13} \text{ cm}^2 \text{ s}^{-1}$) [13, 22] may be smaller than for HCl [39] because of its larger ionic radius and lower ion mobility [40]. The resulting lower surface-to-bulk diffusion rate for HBr compared to HCl allows us to exclude the surface-to-bulk diffusion of HBr being responsible for the very low vapor pressure of HBr over the ice surface.

Conclusion

The kinetics of the uptake of HCl(g) on solid ice surfaces has been studied in a Teflon-coated, low-pressure flow reactor (Knudsen cell) over the temperature range between 190 and 210 K. We separately determined the rate of adsorption and desorption of gaseous HCl on a water ice surface in pulsed dosing and steady state experiments. The kinetics of adsorption depends on the thermodynamic state of the interface: at low HCl partial pressure, the interface is in a quasi-liquid or solid solution state of HCl in ice, and γ of 0.22 at 210 K has been mea-

sured. At high partial pressure, the surface is in a state of liquid HCl/H₂O mixture and $\gamma=0.13$ at 210 K. The HCl/ice system may therefore exist in two distinct regimes under our experimental conditions. We measured a negative activation energy for the "dry" adsorption of HCl of -1.8 ± 0.5 kcal/mol which indicates a complex process. On the other hand, the activation energy for HCl adsorption leading to a liquid solution is -3.1 ± 0.5 kcal/mol, and 5.0 ± 1.5 kcal/mol has been found for the activation energy for HCl desorption. The combination of both processes, adsorption and desorption, is in agreement with literature values of equilibrium vapor pressure taken from the known HCl/H₂O phase diagram. Transient supersaturation and steady state experiments lead to identical results for both the kinetics of adsorption as well as the equilibrium vapor pressure.

The rate of surface-to-bulk loss has been obtained for HCl and HBr using repetitive pulse experiments. For HCl a zero-order limiting rate of 10^{13} and for HBr a rate of $5 \cdot 10^{12}$ molecules $\text{s}^{-1} \text{ cm}^{-2}$ have been found. These values are small with respect to the rate of adsorption and desorption so that we may assert that they do not play a significant role in the interaction of HCl with ice under our present experimental conditions. In the stratosphere the rate of HCl adsorption and surface-to-bulk diffusion are competitive because of the longer time scale and significantly lower HCl partial pressures.

In addition, we measured the retrievable fraction of HCl, defined as the fraction of adsorbed or dissolved HCl which desorbs upon pumping. We found that it depended strongly on the initial concentration of HCl and on temperature, i.e. on the thermodynamic state of the HCl/ice interface. At steady state conditions the retrievable fraction is high ($\sim 80\%$) and low ($\sim 10\%$) for the liquid and quasi-liquid solution, respectively.

The uptake coefficient γ of HCl, HBr and HI on ice have been found to be approximately the same in the temperature range 190 to 210 K for the quasi-liquid state of HX/H₂O. The ice substrate did not support any measurable vapor pressure of HBr or HI after exposure of even large amounts of gas in the range 190 to 210 K.

One of us (B.F.) would like to thank EPFL and Fondation AVINA for support in the framework of the AGS project, "Alliance for Global Sustainability", a collaboration between ETHZ/EPFL, MIT and the University of Tokyo. In addition, the work was supported by a grant from OFES (Office Fédéral de l'Education et de la Science) within the project LEXIS and HALOTROP in the EU Environment and Climate program. We thank Professor H. van den Bergh for his lively interest and support. Illuminating discussions with Professor Mario Molina are gratefully acknowledged. We also thank two anonymous reviewers for their pertinent remarks and helpful suggestions.

References

- [1] S. Salomon, R.R. Garcia, F.S. Rowland, and D.J. Wuebbles, *Nature* 321, 755 (1986).
- [2] M.J. Molina, in: *The Chemistry of the Atmosphere: Its Impact on Global Change*, ed. by J.G. Calvert, Blackwell, Oxford, United Kingdom, 1994.

- [3] D. Hanson and K. Mauersberger, *Geophys. Res. Lett.* **15**, 1507 (1988).
- [4] P.J. Wooldridge, R.Y. Zhang, and M.J. Molina, *J. Geophys. Res.* **100**, 1389 (1995).
- [5] P.N. Krishnan and R.E. Salomon, *J. Phys. Chem.* **73**, 2680 (1969).
- [6] R.G. Seidensticker, *J. Phys. Chem.* **56**, 2853 (1972).
- [7] G.W. Gross, P.M. Wong, and K.J. Humes, *J. Phys. Chem.* **67**, 5264 (1977).
- [8] D.R. Hanson and K. Mauersberger, *J. Phys. Chem.* **94**, 4700 (1990).
- [9] M.J. Molina, R. Zhang, P.J. Wooldridge, J.R. McMahon, J.E. Kim, H.Y. Chang, and K.D. Beyer, *Science* **261**, 1418 (1993).
- [10] E.W. Wolff, R. Mulvaney, and K. Oates, *Geophys. Res. Lett.* **16**, 487 (1989).
- [11] D.R. Hanson and A.R. Ravishankara, *J. Phys. Chem.* **96**, 2682 (1992).
- [12] L.T. Chu and M.-T. Leu, Paper presented at CHEMRAWN VII Conference, 1991.
- [13] E. Thibert and F. Dominé, *J. Phys. Chem.* **101**, 3554 (1997).
- [14] L. Delzeit, B. Rowland, and J.P. Devlin, *J. Phys. Chem.* **97**, 10312 (1993).
- [15] J.D. Graham and J.T. Roberts, *Geophys. Res. Lett.* **21**, 251 (1995).
- [16] A.B. Horn, M.A. Chesters, M.R.S. McCoustra, and J.R. So-deau, *J. Chem. Soc. Faraday Trans.* **88**, 1077 (1992).
- [17] B.J. Gertner and J.T. Hynes, *Science* **271**, 1563 (1996).
- [18] A.R. Ravishankara and D.R. Hanson, *NATO ASI Ser.* **1**, 22, 288 (1994).
- [19] R. Oppliger, A. Allanic, and M.J. Rossi, *J. Phys. Chem.* **101**, 1903 (1997).
- [20] D.G. Johnson, W.A. Traub, K.V. Chance, and K.W. Jucks, *Geophys. Res. Lett.* **22**, 1373 (1995).
- [21] J.P.D. Abbatt, *Geophys. Res. Lett.* **21**, 665 (1994).
- [22] L.T. Chu and J.W. Heron, *Geophys. Res. Lett.* **22**, 3211 (1995).
- [23] S.U. Pickering, *Ber. Dtsch. Chem. Ges.* **26**, 2307 (1893).
- [24] L.T. Chu and L. Chu, *J. Phys. Chem. B* **101**, 6271 (1997).
- [25] T.-L. Shen, P.J. Wooldridge and M.J. Molina, in: *Composition, Chemistry, and Climate of the Atmosphere*, ed. by H.B. Singh, van Nostrand Reinhold, 1995.
- [26] J.P.D. Abbatt, K.D. Beyer, A.F. Fucaloro, J.R. McMahon, P.J. Wooldridge, R. Zhang, and M.J. Molina, *J. Geophys. Res.* **97**, 15819 (1992).
- [27] F. Caloz, F.F. Fenter, K.D. Tabor, and M.J. Rossi, *Rev. Sci. Instrum.* **68**, 3172 (1997).
- [28] F.F. Fenter, F. Caloz, and M.J. Rossi, *J. Phys. Chem.* **98**, 9801 (1994).
- [29] F.F. Fenter, F. Caloz, and M.J. Rossi, *J. Phys. Chem.* **100**, 1008 (1996).
- [30] L.S. Gutzwiler, Thesis no. 1527, Ecole Polytechnique Fédérale de Lausanne, 1996.
- [31] F.F. Fenter, F. Caloz, and M.J. Rossi, *Rev. Sci. Instrum.* **68**, 3180 (1997).
- [32] J.P.D. Abbatt and M.J. Molina, *J. Phys. Chem.* **96**, 7674 (1992).
- [33] S.C. Wofsy, M.J. Molina, R.J. Slawitch, L.E. Fox, and M.B. McElroy, *J. Geophys. Res.* **93**, 2442 (1988).
- [34] M.J. Molina, L.T. Molina, and D.M. Golden, *J. Phys. Chem.* **100**, 12888 (1996).
- [35] L. Chaix and M.J. Rossi, submitted to *J. Phys. Chem.* (1998).
- [36] D.R. Haynes, N.J. Tro, and S.M. George, *J. Phys. Chem.* **96**, 8502 (1992).
- [37] D.E. Brown, S.M. George, C. Huang, E.K.L. Wong, K.B. Rider, R.S. Smith, and B.D. Kay, *J. Phys. Chem.* **100**, 4988 (1996).
- [38] S. Seisel and M.J. Rossi, *Ber. Bunsenges. Phys. Chem.* **101**, 934 (1997).
- [39] A.B. Horn and J. Sully, *J. Chem. Soc. Faraday Trans.* **93**, 2741 (1997).
- [40] D. Barnaal and D. Slotfeldt-Ellingsen, *J. Phys. Chem.* **87**, 4321 (1983).

(Received: March 20, 1997
final version: April 16, 1998)

E 9528